

Dielectric Stimulated Arc Breakdown Across a Spark Gap for Surge Protection

Pin Yang*, John K. Grey, David E. Vreeland, and Josef D. Sorenson

Electronic, Optical, and Nano Materials, Sandia National Laboratories

*Albuquerque, New Mexico, USA

*e-mail: pyang@Sandia.gov

The introduction of high dielectric permittivity ceramic granules in a spark gap geometry can divert surge currents by significantly reducing the breakdown voltage and narrowing its distribution. This work demonstrates a practical application for surge protection and reviews basic concepts of dielectric stimulated arc breakdown at lower voltages. Key factors such as dielectric constant and gas pressure on the fast-rise breakdown in a dielectric filled spark gap will be reported and discussed.

Key words: Surge Protection, Dielectric Stimulated Arc, Fast Rise Breakdown

1. INTRODUCTION

High power surges can pose a serious threat to electrical systems.[1] Effective diversion of power surges is vital to prevent unwanted damage to sensitive electronics. Dielectric stimulated arc breakdown is a fast, effective, and self-healing mechanism that can quickly divert unexpected surges to ground and mitigate damage. The mechanism lowers the breakdown threshold voltage and current density since the resistance of the arc plasma increases with decreasing electric potential.[2]

This paper reviews the basic concepts of dielectric stimulated arc breakdown across a spark gap [2][3] and demonstrates the importance of dielectric permittivity of ceramic granules in lowering the breakdown voltage for surge protection.[4] Effects of gas pressure on the arc breakdown will be also reported.

1.1 Paschen Breakdown

Arc breakdown due to discharge across an air gap is governed by the ability to ionize gas molecules under the influence of an electric field according to the Paschen's law.[5][6] The breakdown voltage with respect to the product of gap width (d) and pressure (p) is generally referred as the Paschen curve. An example of the Paschen curve for gas discharge in air between two parallel plates is illustrated in Fig. 1.

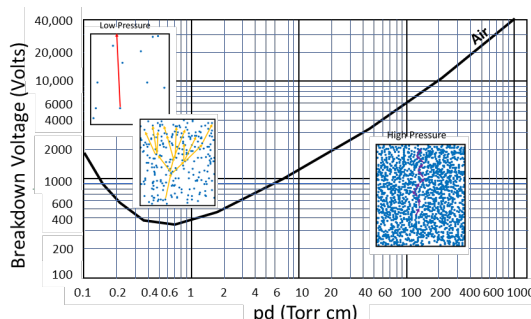


Fig. 1. Paschen curve of air under ambient temperature.

For a fixed gap space (d), as in the case study for this paper, the response on the horizontal axis can be interpreted as changing in gas pressure. On the left-hand side, at the low gas pressures, the probability of

encountering gas molecules are low and the electron mean free path (l_e) is large. Therefore, there is insufficient ionization events (or ionization density) causing ionization multiplication and only partial discharge is possible. As a result, the breakdown voltage (V_b) is near its upper limit on the left due to the stochastic nature of few individual partial discharges. Increasing pressure reduces l_e resulting in greater collisional encounter frequencies. If electrons can gain sufficient energy in their trajectories and are able to ionize gas molecules, the condition becomes more favorable for ionization amplification. V_b decreases and continues until reaching a minimum on the Paschen curve. As gas pressure increases further, due to the increase in collisions frequency, smaller l_e values limit achievable electron kinetic energy and therefore reduce ionization multiplication yields. Breakdown becomes mechanically limited. This situation causes V_b to increase with pressure. These scenarios and relative l_e values are illustrated in these insert drawings in Fig. 1. The blue dots and arrows are representing the gas molecules and l_e , respectively.

1.2 Field Splitting Due to Dielectric Insertion

The insertion of a higher permittivity dielectric to the air gap concentrates the electric field across the air gap. A simple illustration is given in Fig. 2, where the thickness of the insert dielectric medium (d) and the spacing of air gap are kept the same and both media share the same contact area (A). Under this condition, the total charge (Q) at the air and dielectric interface under applied voltage (V_{total}) remains the same, so

$$Q = C_{Air}V_{Air} = C_{Dielectric}V_{Dielectric} \quad (1)$$

The change of the ratio of the voltage across the air gap (V_{air}) and the total applied voltage (V_{total}) with respect to the dielectric permittivity of the dielectric is plotted in Fig. 2. For dielectrics of different thickness, the electric field ($E = V/d$) will be splitting between air and dielectric according the following relationship,

$$E_{Air} \epsilon_{Air} = E_{Dielectric} \epsilon_{Dielectric} \quad (2)$$

As the dielectric permittivity (ϵ) of the dielectric increase, field or voltage will be concentrated in air ($\epsilon_{\text{Air}} = 1$). Illustrated in Figure 2, the electric field or voltage (blue curve) increases drastically across the air gap when the relative dielectric permittivity of the dielectric below 100 and beyond this value towards an asymptotic limit.

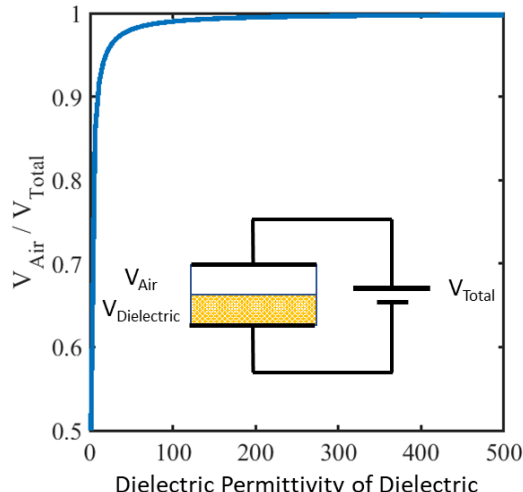


Fig. 2. Change of voltage (or electric field) distribution as a function of dielectric permittivity of the inserted dielectric based on a simple parallel plate capacitor.

When high permittivity ceramic granules are introduced, the electric potential in the spark gap will be strongly distorted. For simplicity, such a distortion is illustrated by a two dimensional simulation of a single (idealized) granule between two parallel plates with isopotential contour lines depicting the electric field across two parallel plates (Fig. 3 (a)).

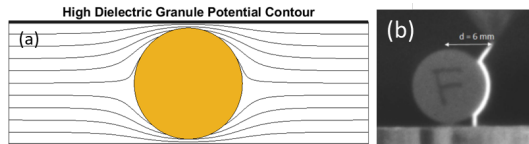


Fig. 3. (a) Distortion of the isopotential contour lines due to the introduction of a high dielectric constant granule across an air gap, (b) experimental observation of the influence of field distortion on arc breakdown path.

Note that the contour lines in Fig. 3 (a) become “squeezed” in the vicinity of the granule and parallel plates. As a result, the local potential gradient (or E) between metal plates and dielectric granule increases dramatically. This localized field concentration can be demonstrated by the changing or arc path in Fig. 3 (b) captured by a high speed camera.[7] This image shows that an arc initiated from a sharp tip on the right side propagates orthogonally through the steepest potential descent in the “squeezed” region to the dielectric surface then continue its path to the ground.

As the result of the localized electric field concentration, kinetic energy of primary electron precursors from Townsend discharge will increase and ionized species in the spark gap, enhance the gas

ionization rates ($\alpha \sim \exp(-1/E)$) for ionization multiplication, and reduce the breakdown voltage and narrow its distribution.

2. EXPERIMENTAL PROCEDURE

The lead magnesium niobate-lead titanate (PMN-PT) ceramic powder was synthesized by a solid-state reaction between 50 mol.% of PMN (Tamtron) and 50 mol.% PT (Ferro) powders at 750°C for 4 hours. Green compacts were uniaxially pressed then isostatically pressed to 30 ksi. Some pressed compacts were pulverized into granules. These compacts and granules were sintered in double inverted crucibles at 1050°C for 90 minutes to form dense ceramics (> 97 % of theoretical density). Ceramic granules were sieved between 70 mesh (210 μm opening) and 100 mesh (149 μm opening) for arc breakdown measurements. Sintered pellets were ground and sputtered with Cr/Au electrodes. The dielectric constant of the sintered pellet was measured in an environmental testing chamber from room temperature to 325°C with a LCR meter (Keysight E4980AL) at 10 kHz.

Fast-rise breakdown (FRB) was measured by an amplified square pulse > 1200V with 300 ns to 1 μs pulse width. The voltage ramp rate was adjusted by a pulse shaping network to be as close as possible to 10 kV/ μs to simulate a fast rising surge condition.[8] Traces of the trigger pulse and voltage waveform across the PMN-PT granule filled spark gap were digitally recorded by an oscilloscope (Agilent, Infini Vision DSO6054A) and analyzed by a MATLAB program. The maximum surge voltage and voltage ramp rate were determined from voltage/current waveforms of 21 consecutive shots to ensure statistical reliability and average values and standard deviation were compared and analyzed. For temperature dependent measurements, breakdown data were collected continuously with a five-second interval between each shot to de-energize and relax residual ionized species between the spark gap. A schematic layout of the test system was reported elsewhere.[9]

3. RESULTS AND DISCUSSION

3.1 Fast Rise Breakdown and Waveforms

Typical FRB waveforms including the voltage and the current traces for a PMN-PT filled spark gap are illustrated in Fig. 4. The insert in Fig. 4 (a) is a cartoon representation of the annulus shape spark gap used in this investigation where high permittivity granules are filled in a 0.03 cm gap between the central pin and outside ring.

The FRB is distinguished by a quick linear rising potential to the peak voltage followed by sharp decrease and change of sign as shown in Fig. 4(a). The hallmark of a dielectric induced arc breakdown is further confirmed by comparing the current response (Fig. 4 (b)) where a large current spike at breakdown initiation (voltage drop) consistent with complete gas discharge. FRB voltage (V_{FRB}) is evaluated from the maximum of the transient response and the ramp rate is quantified by measuring the voltage rise slope between 50-80% of the maximum. The subsequent ringing in these waveforms is a result of oscillations from the pulse shape network used in the test circuit. These features do not change appreciably from

pulse-to-pulse making it possible to reliably discern differences between each event.

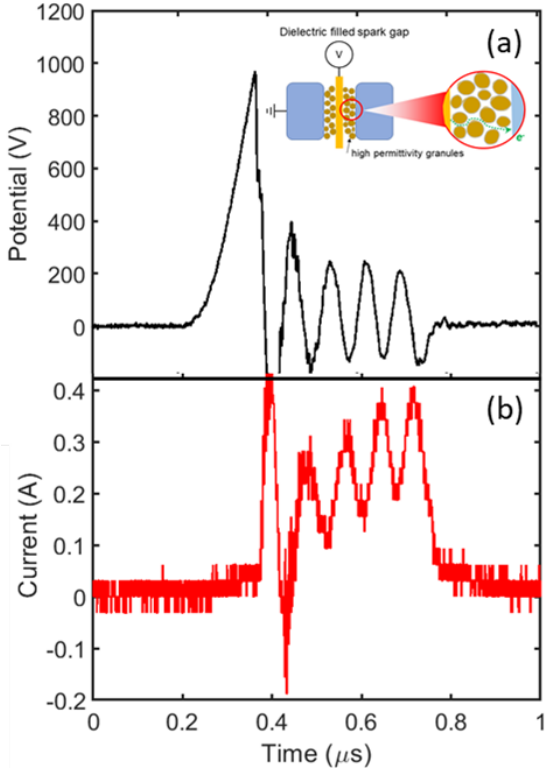


Fig. 4. (a) Voltage and (b) current waveforms obtained from a fast-rise breakdown,

3.2 Paschen Curve for Dielectric Filled Spark Gap

Although there are many studies on gas discharge with simple parallel plate capacitor-type geometry with DC applied voltages, only one study reported the gas breakdown with inserted ceramic granules.[10] For the current annulus test configuration, the average breakdown voltage (21 shots) versus pressure under 1250 V pulses are given in Fig. 5. Generally speaking, the shape of the Paschen curve is similar to Fig. 1, except the breakdown voltages are lower so the change in breakdown voltage with respect to pressure (or slope) in the mechanically limited region is much steeper. Due to the limitation imposed by l_e in the mechanically limited region, the standard deviation of the breakdown voltage is smaller than data collected in the stochastic range on the right.

Data indicate that near ambient condition the breakdown voltage for the 300 μm annulus shape spark gap is about 1150 ± 45 V, and the Paschen minimum is around 25 Torr. The results indicate that the breakdown response of a dielectric filled spark gap is still governed by the same mechanisms described by Paschen's law.

3.3 Dielectric Constant and Fast-rise Breakdown Voltage

The change of dielectric constant versus temperature for the PMN-PT pellet was measured at 10 kHz and data were plotted on the right Y axis in Fig. 6. The result shows the Curie temperature (T_c) for this PMN-PT composition is at 252°C where the dielectric constant reaches a

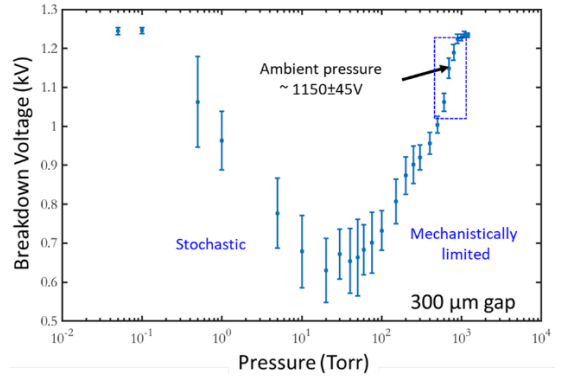


Fig. 5. The Paschen behavior of a PMN-PT filled, annulus shape spark gap measured by 1250 V pulses at room temperature.

maximum of 20707. Above T_c , the spontaneous polarization disappears as the ferroelectric phase transforms into its paraelectric state. The left axis depicts the temperature-dependent V_{FRB} trend under 760 Torr (1 atm) and 1900 Torr (2.5 atm) conditions. The two sets of data show a similar trend where the V_{FRB} decreases monotonically to the minimum point at the T_c , then increases as temperature increases. The general up shift in the breakdown voltage data sets between these measurements is consistent with Paschen's law in the mechanically limited region (Fig. 5).

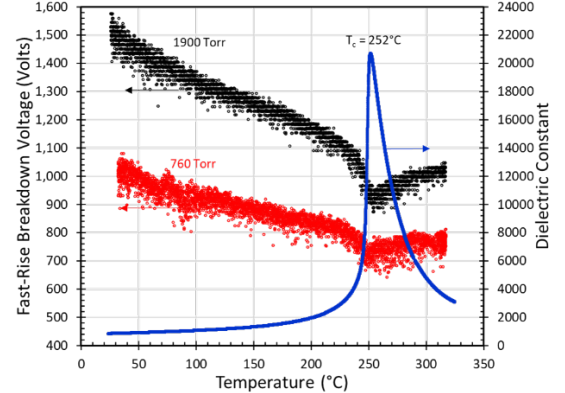


Fig. 6. Temperature dependence of V_{FRB} and dielectric constant for granule filled spark gap and pellet made from PMN-PT ceramic. Data were collected by 2000 V fast-rise pulses under different pressures.

Near the Curie temperature, the decrease in V_{FRB} is steeper for data collected at 1900 Torr than those at 760 Torr. The steeper change in both conditions are related to the rapid change in dielectric constant which greatly enhances the local field in the air pockets and increases the probability of initiation of arc breakdown. The difference can be attributed to how these ionized species (mostly electrons in a fast-rise pulse)[11] reaching criticality of ionization multiplication to initiate an arc breakdown. At 1900 Torr l_e is shorter and ionized species due to Townsend partial breakdowns are closely packed in comparison to the condition at 760 Torr. Such a condition is favorable for triggering the avalanche breakdown at lower voltages. As a result, the change in breakdown voltage is greater under the same field enhancement, resulting a steeper slope on Fig. 6. As the

temperature increases above 230°C where the dielectric constant changes drastically and local field enhancement approaches to the asymptotic point, ionization density would increase more and further lowering the V_{FRB} near the Curie temperature. The higher the ionization density, the more pronounced the effect. This lead a steeper decrease in V_{FRB} (or slope) for measurement under 1900 Torr.

3.4 Field Concentration and Pressure on Gas Discharge

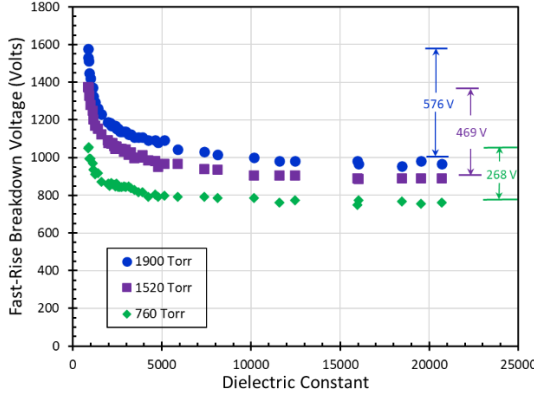


Fig. 7. Change in fast-breakdown voltage versus dielectric constant of PMN-PT under different pressures.

Fig. 7 plots the change of V_{FRB} with respect to the dielectric constant of PMN-PT under three different pressure conditions. The dielectric data are compiled from the temperature dependent measurements on both sides of the Curie point on Fig. 6. These curves illustrate the effect of field concentration due to dielectric constant change to the V_{FRB} . The shape of these curves is unique to the annulus shape test fixture, and may vary with the shape, size and distribution of dielectric granules.[12] Although the onset toward the asymptotic limit (dielectric constant > 5000) for these measurements is somewhat greater than predicted in Eq. 2, the behavior is overall consistent with expectation from the parallel plate capacitor model. The upshift of the V_{FRB} curve with testing pressure follows Paschen's law in the mechanically limited region. Similar to the argument used in the previous section (Section 3.3), the increase in ionization density due to gas pressure helps bring down the breakdown voltage. This effect leads greater change in V_{FRB} for the dielectric constant between 1000 to 5000 in these high pressure measurements as indicated by the data reported on the right in Fig. 7. These results also indicate that arc breakdown can be consistently triggered below 1000 volts below 2.5 atmospheres if the dielectric constant of the ceramic granules exceeds 10,000.

4. CONCLUDING REMARKS

From the change of dielectric constant of PMN-PT as function of temperature and the change of breakdown voltage with respect to pressure, the important contribution of high permittivity ceramic granules on arc breakdown in a spark gap is demonstrated, which serves as the technical basis for surge protection design. Results indicate that the extent of field concentration due to the introduction of the granules dictates the lowest breakdown voltage. The arc breakdown in a dielectric

filled spark gap still follows the Paschen's law with a breakdown minimum below the ambient pressure. Experimental observation further indicates that ionization density plays a key role on fast-rise breakdown. When gas pressure is below the Paschen minimum where ionization density is low and breakdown is stochastic, the standard deviations of the breakdown voltage are greater. As pressure increases where breakdown becomes mechanically limited, the standard deviations will progressively become smaller. The field enhancement on arc breakdown become more pronounced at high pressure due to the increase in ionization density that tends to trigger avalanche breakdown and lower the breakdown voltage.

5. ACKNOWLEDGEMENT

Sandia National Laboratories is a multi-mission laboratory managed and operated by National Technology and Engineering Solutions of Sandia, LLC, a wholly owned subsidiary of Honeywell International Inc., for the U.S. Department of Energy's National Nuclear Security Administration under contract DE-NA0003525. SAND No. SAND2022-13341 C.

6. REFERENCES

- [1] J. R. Dwyer and M. A. Uman, *Phys. Rep. Phys. Lett.*, **534**, 147-241 (2014).
- [2] k. Brainard and L. Andrew, *IEEE Trans. Compon. Hybrids Manuf. Technol.*, **2**, 309-316 (1976).
- [3] J. A. Cooper and K. J. Allen, *IEEE Trans. Electromagnetic Compat.*, **ECM-15** [3], 104-110, (1973).
- [4] P. Yang, J. D. Sorenson, C. A. Gomez, M. A. Bleakirby, and W. C. Moffatt, *J. Appl. Phys.*, **128**, 094103 (2020).
- [5] P. Mathew, J. George, S. Mathews, T. and P. J. Kurian, *AIP Advances*, **9**, 025215 (2019).
- [6] L. Lisovskiy, S. Yakovin, and V. Yegorenkov, *J. Phys. D Appl. Phys.*, **33**, 2722 (2000).
- [7] K. M. Williamson, S. Simpson, R. S. Coats, R.E. Jorgenson, H. P. Hjalmarson, P. Harold, M. F. Pasik, SAND2013-8729, Sandia National Laboratories (2013).
- [8] M. A. Uman and V. A. Rakov, *Science*, **246**, 457-464 (1989).
- [9] P. Yang, C. A. Gomez, S. Andrews, J. D. Sorenson, and K. S. Chen, *J. Am. Ceram. Soc.*, **104**, 3247-3259 (2020).
- [10] C. Colson, "PMN/PT and rutile LAC voltage breakdown dependency with respect to backfill gas, voltage rates, and Pressure," Master Thesis, Electrical and Computer Engineering, University of New Mexico, (2011)
- [11] D. Levko, R. R. Arslanbekov, and V. I. Kolobov, *Plasmas*, **26**, 064502 (2019).
- [12] P. Shepherd, D. Thomas, I. Harrison, R. Lynch, L. Clark, S. de La Bedoyre, E. Hadzifejzovic, and D. Gregory, 29th Int. Conf. Lightning Protection, Uppsala, Sweden, 23-25 (2008).